Pure appl. geophys. 161 (2004) 1453–1467
0033–4553/04/071453–15
DOI 10.1007/s00024-004-2514-5

Pure and Applied Geophysics

The Interpretation of Gravity Changes and Crustal Deformation in Active Volcanic Areas

M. BATTAGLIA[1,2], and P. SEGALL[1]

Abstract — Simple models, like the well-known point source of dilation (Mogi's source) in an elastic, homogeneous and isotropic half-space, are widely used to interpret geodetic and gravity data in active volcanic areas. This approach appears at odds with the real geology of volcanic regions, since the crust is not a homogeneous medium and magma chambers are not spheres. In this paper, we evaluate several more realistic source models that take into account the influence of self-gravitation effects, vertical discontinuities in the Earth's density and elastic parameters, and non-spherical source geometries. Our results indicate that self-gravitation effects are second order over the distance and time scales normally associated with volcano monitoring. For an elastic model appropriate to Long Valley caldera, we find only minor differences between modeling the 1982–1999 caldera unrest using a point source in elastic, homogeneous half-spaces, or in elasto-gravitational, layered half-spaces. A simple experiment of matching deformation and gravity data from an ellipsoidal source using a spherical source shows that the standard approach of fitting a center of dilation to gravity and uplift data only, excluding the horizontal displacements, may yield estimates of the source parameters that are not reliable. The spherical source successfully fits the uplift and gravity changes, overestimating the depth and density of the intrusion, but is not able to fit the radial displacements.

Key words: Volcano geodesy, gravity, crustal deformation, calderas, models.

1. Introduction

Quite simple models are widely used to interpret geodetic and gravity data in active volcanic areas. An example is the well-known point source of dilation (Mogi's source), used to approximate the behavior of a pressurized spherical magma chamber, embedded in an elastic, homogeneous, and isotropic half-space (EGGERS, 1987; DVORAK and DZURISIN, 1997). Mogi's source models successfully reproduce displacement and gravity changes at many volcanoes during either uplift or subsidence (MCKEE *et al.*, 1989; BERRINO, 1994; BATTAGLIA *et al.*, 1999). In addition, some authors use the linear gravity/height correlation from the point source model to study the physics of magma chambers (RYMER and WILLIAM-JONES, 2000) or investigate the likelihood of volcanic eruptions (BERRINO *et al.*, 1992; RYMER,

[1] Department of Geophysics, Stanford University, Stanford CA 94305-2215, U.S.A.
[2] Corresponding author. Now at: Seismo Lab, UC Berkeley, 215 McCone Hall, Berkeley CA 94720-4760, U.S.A. E-mail: battag@seismo.berkeley.edu

1994). This approach appears at odds with the complex geology of volcanic regions, since the crust is not a homogeneous medium and magma chambers are not spheres. But what should a model include to obtain a better insight into the physics of volcanoes? Some authors claim that elastic-gravitational models can be a far more appropriate approximation to problems of volcanic load in the crust than the more commonly used purely elastic models (e.g., RUNDLE, 1982; FERNÁNDEZ *et al*., 2001a, 2001b). Vertical discontinuities in the Earth's density and elastic parameters can play an important role when modeling gravity changes induced by deformation (FERNÁNDEZ et al, 1997; BONAFEDE and MAZZANTI, 1998). We apply models including one (or more) of the above features to the 1982–1999 period of unrest at Long Valley caldera to evaluate: (a) if elasto-gravitational models are a more appropriate approximation to problems of volcanic load in the crust than the purely elastic models at the space and time scales associated with volcano monitoring; (b) the importance of vertical discontinuities in the Earth's density and elastic parameters when modeling displacement and gravity changes induced by a point source of dilation; (c) the bias introduced using a point source of dilation model to reproduce geodetic and gravity data if the magma intrusion does not posses a spherical symmetry.

Our results show that (a) self-gravitation effects due to coupling between elasticity and gravity potential are second order over the distance and time scales normally associated with volcano monitoring. (b) For an elastic model appropriate to Long Valley caldera, we find only minor differences between modeling the intrusion using a point source in a homogeneous or layered medium. (c) A simple experiment of matching deformation and gravity data from an ellipsoidal source (YANG *et al*., 1988; CLARK *et al*., 1986) using a spherical source suggests that the standard approach of fitting a center of dilation to gravity and uplift data only, excluding the horizontal displacements, can yield estimates of the source parameters that are not reliable. In our experiment, the spherical source successfully fits the uplift and gravity changes, inferring a deeper location (8.5 km instead of 6 km) and a larger density (4500 kg/m^3 instead of the actual 2500 kg/m^3) for the intrusion, but is not able to fit the radial displacements.

2. Coupling between Elastic and Gravitational Effects

The complete solution for gravity and deformation changes in volcanic regions should include the coupled effects of gravity and displacement changes (FERNÁNDEZ *et al*., 1997). To determine if these effects are important on space and time scales associated with volcano monitoring, we perform a dimensional analysis of the fully coupled elasticity and potential equations (see POLLITZ, 1997 for similar discussion in the earthquake context). We approximate the Earth with an isotropic, elastic sphere. The origin of the coordinate system is taken at the center of this sphere. Following

the approach by LOVE (1911, p. 89), the density ρ_0, the pressure p_0 and the potential V_0 (with the corresponding gravitational acceleration $-g_0\mathbf{e}_r = \nabla V_0$ define the initial state of equilibrium

$$\rho_0 \nabla V_0 = \nabla p_0. \tag{1}$$

After the intrusion of mass in a spherical magma body of initial radius a (approximated by the superposition of a point source of dilation and a mass point source at $\mathbf{x} = \mathbf{x}_m$, see Fig. 1), the Earth's surface deforms by $\mathbf{u}$ ($|\mathbf{u}| \ll a$). Perturbations in the density ρ, pressure p and potential V are defined by

$$\begin{aligned} \rho &= \rho_0 - \nabla \cdot (\rho_0 \mathbf{u}) \\ p &= p_0 - \mathbf{u} \cdot \nabla p_0 \\ V &= V_0 + V_p + V_m \end{aligned} \quad , \tag{2}$$

where V_p is the change in the Earth's potential due to inflation of a massless cavity and V_m is the potential due to the mass $\Delta M = \rho_m \Delta V$ of the intrusion (ρ_m and ΔV are respectively the density and volume of the intrusion). The equilibrium equation is

$$\nabla \cdot \mathbf{s} - \nabla p + \rho \nabla V + \mathbf{F}_p + \mathbf{F}_m = 0, \tag{3}$$

where $\mathbf{s}$ is the elastic stress tensor, $\mathbf{F}_p$ and $\mathbf{F}_m$ are the body force density corresponding to a point source of dilation and a mass point source. Substituting

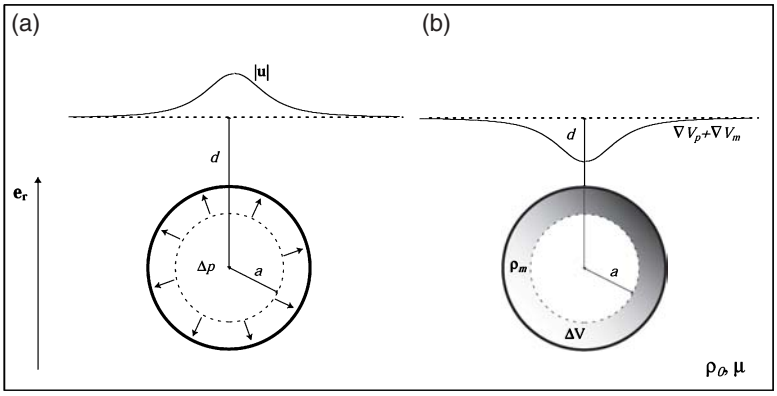

Figure 1
Coordinate system and parameters for the scaling problem. The effect of a magma body intrusion is approximated by two contributions: (a) a pressurized mass-less cavity; (b) a spherical mass intrusion with no pressure change. Scaling parameters (Table 1): u — vertical displacement; ρ_0 — crust density; μ — shear modulus; d — depth of the magma chamber; a — radius of the magma chamber; ρ_m — magma intrusion density; ΔP — pressure change; ΔV—volume change; $\nabla V_p + \nabla V_m$—changes in gravity, see (2).

(2) in (3), we get the following equations describing the potentials V_p and V_m, and the elastic deformation (RUNDLE, 1982)

$$\nabla^2 V_p = 4\pi G \nabla \cdot (\rho_0 \mathbf{u}), \quad \nabla^2 V_m = -4\pi G \rho_m \delta(\mathbf{x} - \mathbf{x}_m) \tag{4}$$

$$\nabla \cdot \mathbf{s} - g_0[\nabla(\rho_0 \mathbf{u} \cdot \mathbf{e}_r) - \mathbf{e}_r \nabla \cdot (\rho_0 \mathbf{u})] + \rho_0 \left[\nabla V_p + \nabla V_m\right] + \mathbf{F}_p + \mathbf{F}_m = 0. \tag{5}$$

The second and third term on the left-hand side of (5) depend on g_0. The fourth and fifth term on the left-hand side of (5) depend on G. The g_0 dependent part scales as $g_0 \rho_0 u/d$, where u and d are characteristic distance scales set respectively by the vertical displacement and the depth of the magma chamber. From (4), ∇V_p scales as $G\rho_0 u$. The scaling of ∇V_m is given by the expression for the gravity change associate to a mass point source, $G\rho_m \Delta V/d^2$ (EGGERS, 1987). The elastic stress s scales as $\mu u/d$ .The shear modulus μ is most commonly estimated from seismic wave speeds. However, the dynamic modulus (μ_d) may exceed the quasi-static shear modulus (μ_s). The ratio μ_d/μ_s depends on several factors including the porosity and applied pressure p. For granite and tuff (CHENG and JOHNSTON, 1981), $\mu_d/\mu_s \approx 0.1$ at low pressures ($p \leq 0.1$ GPa, depth ≤ 3.5 km) and $\mu_d/\mu_s \approx 1$ when $p \geq 0.2$ GPa (depth ≥ 7.0 km).

Using typical parameter values (see Table 1), we can show that the potentials V_p and V_m have the same order of magnitude, but are negligible compared to the elastic term

$$\frac{\nabla V_p}{\nabla V_m} \sim \frac{ud^2}{\Delta V} \sim 1, \quad \frac{\rho_0 \nabla V_p}{\nabla \cdot \mathbf{s}} \sim \frac{G\rho_0^2 d^2}{\mu} \sim 10^{-5}. \tag{6}$$

A similar scaling analysis for the relative importance of g_0 and elastic terms gives

$$\frac{g_0[\nabla(\rho_0 \mathbf{u} \cdot \mathbf{e}_r) - \mathbf{e}_r \nabla \cdot (\rho_0 \mathbf{u})]}{\nabla \cdot \mathbf{s}} \sim \frac{\rho_0 g_0 d}{\mu} \sim 10^{-2} \tag{7}$$

that indicates that g_0 terms are negligible as well. $\mathbf{F}_p$ scales as

$$F_p \sim \frac{\left|\mathbf{M}_p \nabla \delta(\mathbf{x} - \mathbf{x}_m)\right|}{\Delta V} \sim \frac{\lambda + 2\mu}{\mu} \frac{\pi a^3 \Delta P}{a} \frac{1}{\Delta V} \sim \frac{\mu}{a}, \tag{8}$$

where $\mathbf{M}_p \nabla \delta(\mathbf{x} - \mathbf{x}_m)$ is the body-force equivalent to a point source of dilation (AKI and RICHARDS, 1980, p. 61), λ and μ are the elastic moduli, ΔP the pressure change of

Table 1

Value of scaling parameters. The volume change ΔV corresponding to a vertical displacement u is estimated using a point source model (EGGERS, 1987)

d m	ρ_0, ρ_m kg/m^3	u m	μ Pa	ΔV m^3	a M
10^3	$3{\cdot}10^3$	1	$3{\cdot}10^9$	10^6	10^3
10^4	$3{\cdot}10^3$	1	$3{\cdot}10^{10}$	10^8	10^3

the point source of dilation and δ the Dirac's delta function. $\mathbf{F}_m$ scales as (ZHONG and ZUBER, 2000)

$$\mathbf{F}_m = -\rho_m g_0 \delta(\mathbf{x} - \mathbf{x}_m)\mathbf{e}_r \sim \rho_m g_0. \tag{9}$$

The ratio between the two body-forces gives

$$\frac{\mathbf{F}_m}{\mathbf{F}_p} \sim \frac{\rho_0 g_0 a}{\mu} \sim 10^{-2}. \tag{10}$$

$\mathbf{F}_p$ is larger than $\mathbf{F}_m$ and the equilibrium equation (5) reduces to

$$\nabla \cdot \mathbf{s} + \mathbf{F}_p = 0. \tag{11}$$

In summary, we can see from (6), (7) and (10) that the coupling between gravity and elasticity is negligible in the space scale associated with volcano monitoring. Changes in the spherical magma body pressure push the deformation, while the potential V_p (due to coupling between gravity and deformation) is of the same order of magnitude as the potential V_m (due to mass intrusion). It is worth noting that in the special case of a spherically symmetric source in a homogeneous medium, RUNDLE (1978) and WALSH and RICE (1979) show that the change in gravity actually results only from the mass of the intrusion. That is, the change in gravity due to coupling between gravity and deformation cancel ($|\nabla V_p| = 0$). We will further investigate in the next section the coupling between elasticity and gravity.

3. Layered Earth Model

In the second step of our investigation into the interpretation of gravity and deformation changes, we will compare estimates of the parameters (depth, volume, mass, density) of the deformation source both for a homogeneous and layered half-space model of Long Valley caldera, California (Fig. 2 and Fig. 3). The goal is to evaluate the various deformation models including elasto-gravitational effects and vertical discontinuities in the Earth's density and elastic parameters (e.g., FERNÁNDEZ *et al.*, 2001a). We also check the results of the dimensional analysis performed in Section 2.

Over the past two decades, Long Valley caldera has shown persistent unrest with recurring earthquake swarms, uplift of the resurgent dome by over 80 cm and the onset of diffuse magmatic carbon dioxide emissions around the flanks of Mammoth Mountain on the southwest margin of the caldera (BAILEY and HILL, 1990, SOREY *et al.*, 1993; LANGBEIN *et al.*, 1995). Several sources of deformation have been identified in Long Valley caldera, although their geometry, depth and volume are not yet well constrained. Surveys of two-color EDM and leveling networks indicate that the principal sources of deformation are the intrusion of a magma body beneath the resurgent dome, and right lateral strike-slip within the

south moat of the caldera (LANGBEIN *et al.*, 1995). In addition, there is evidence for dike intrusion beneath the south moat (SAVAGE and COCKERHAM, 1984) and Mammoth Mt. (HILL *et al.*, 1990). The intrusion beneath the resurgent dome has been confirmed by gravity measurements (BATTAGLIA *et al.*, 1999). For the purpose of this work, we will use uplift and residual gravity data collected in Long Valley caldera between 1982 and 1999.

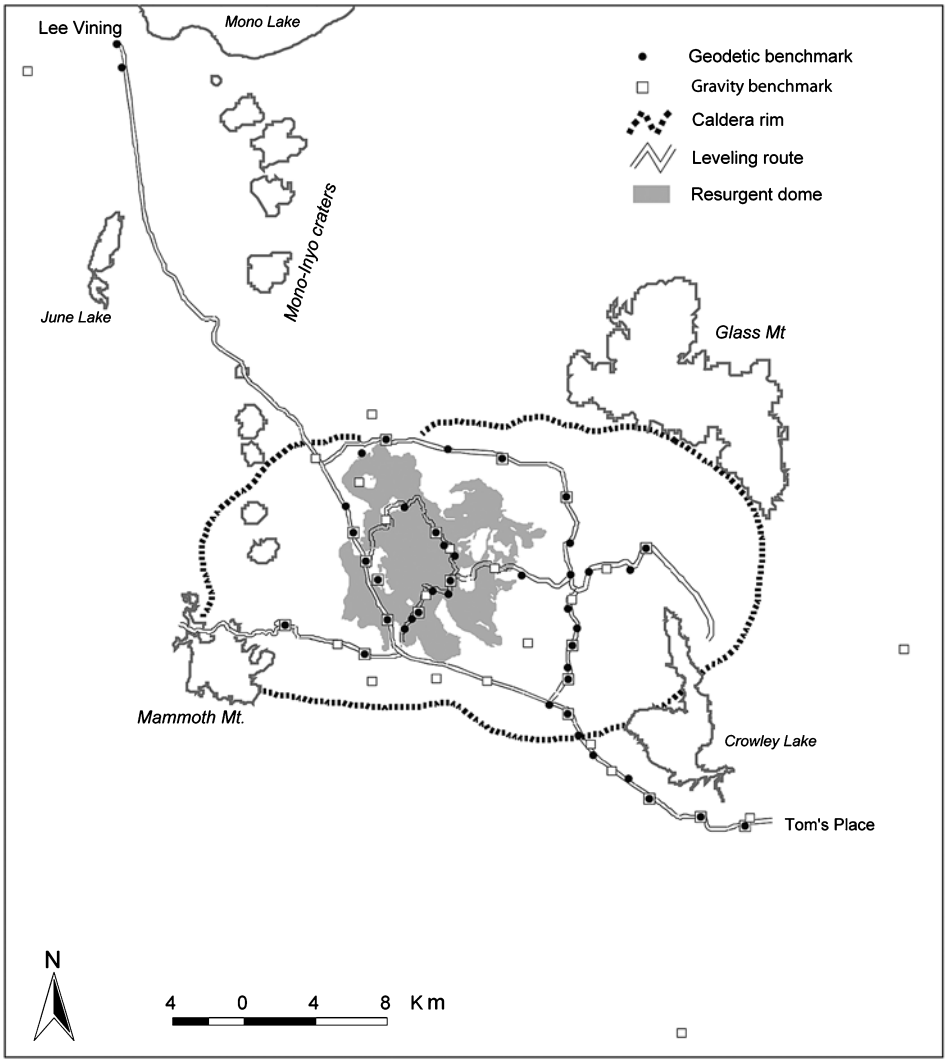

Figure 2
Map of Long Valley showing the location of the leveling and gravity benchmarks.

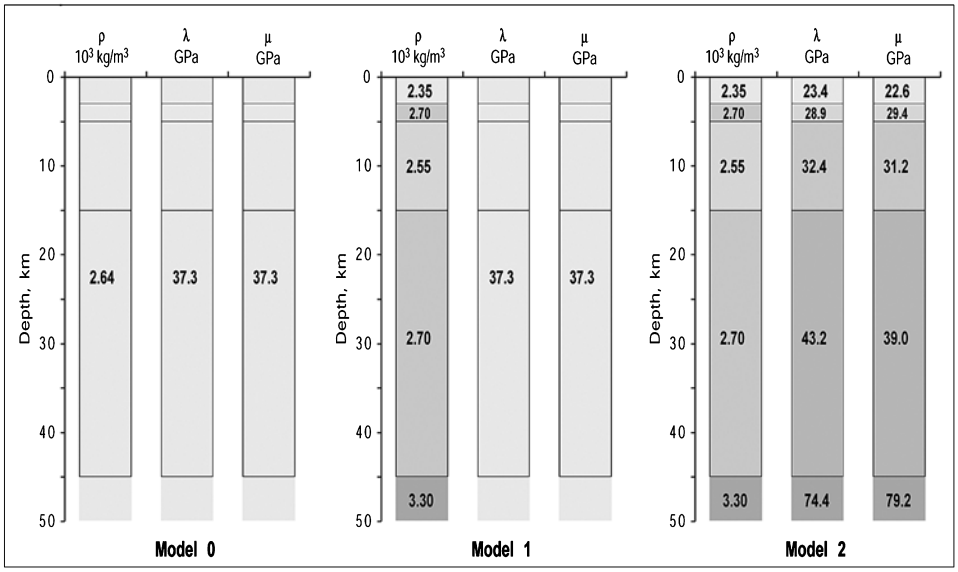

Figure 3
The layered model proposed to study gravity and deformation changes in Long Valley caldera (see Table 2). Model 0 represents a homogeneous medium with average values of the parameters; *Model 1* is elastically homogeneous, but with density stratification; *Model 2* is elastically inhomogeneous.

The Earth model proposed for Long Valley caldera includes 5 layers, the fifth being the mantle (see Table 2, Fig. 3). The thickness, density and seismic velocities assigned to the four layers representing the crust have been estimated from published works on regional gravity, seismic tomography and geology of Long Valley (KISSLING *et al.*, 1984; CARLE, 1988; DAWSON *et al.*, 1990; PONKO and SANDERS, 1994; SACKETT *et al.*, 1999). We use the numerical code developed by FERNÁNDEZ *et al.* (1997) to compute gravity changes and deformation due to an isotropic point source of dilation in a layered half-space. This code solves the fully coupled system of elastic-gravitational equations. Gravity changes and deformation due to a spherical intrusion in a homogeneous half-space are computed using the analytical point source approximation (EGGERS, 1987).

The numerical experiments are carried out considering separately (i) the effects on gravity changes and uplift due to a pressurized magma chamber cavity with no mass change and (ii) the effects of mass intrusion only with no magma chamber overpressure. Note that individually (i) and (ii) do not possess a geologic equivalent, because the geologically meaningful solution is given by the superposition of (i) and (ii). Furthermore, to study the effect of the density and elastic moduli stratification, we consider three different cases (see Fig. 3): (a) homogeneous medium (*Model 0*); (b) density stratification in an elastically homogeneous medium (*Model 1*); (c) an elastically inhomogeneous medium (*Model 2*). The results of the numerical

Table 2

Layered model of Long Valley caldera (see Fig 3b). Crosssection modified after SACKETT *et al., (1999), density model after* CARLE *(1988), velocity model after* KISSLING *et al., (1984), depth of the Moho after* DAWSON *et al., (1990)*

Layers	Crosssection	Thickness km	Depth Km	Density Model 10^3 kg/m^3	Velocity model 10^3 m/s		λ_d GPa	μ_d GPa
					V_S	V_P		
1	Caldera fill bishop tuff	3	3	2.35	3.1	5.4	23.4	22.6
2	Basement	2	5	2.70	3.3	5.7	28.9	29.4
3	Solidified magma chamber	10	15	2.55	3.5	6.1	32.4	31.2
4	Basement	30	45	2.70	3.8	6.7	43.2	39.0
5	Mantle			3.30	4.9	8.4	74.4	79.2
0	Homogeneous model	45		2.64			37.3	

computation for the homogeneous medium are compared with the analytical results. For every one of the seven (six numerical and one analytical) experiments, we find the solution that best fits the gravity and deformation data from Long Valley caldera using a least squares algorithm. To compare the results, we use two quantitative indicators:

$$\chi^2 = r^T \Sigma^{-1} r, \quad R^2 = 1 - \frac{r^T \Sigma^{-1} r}{u^T \Sigma^{-1} u}, \tag{12}$$

where r is the difference between the observed and predicted displacements, and Σ the data covariance matrix, u is the observed displacements. χ^2 is a measure of the error in fitting the experimental data with a model (the smaller χ^2 the better the fit), while R^2 is a measure of the ability of the model to explain the data. If $R^2 = 1$, the model is able to explain all variations in the observed data, if $R^2 = 0$, the model cannot explain the observed data.

For a pressurized mass-less cavity, the fit of the computed uplift to the Long Valley data differs significantly for the three different structural models (Fig. 4a, Table 3). The only noticeable difference is the slightly deeper source (9.4 km instead of 8.8 km, a 7% increase) obtained for the elastically inhomogeneous medium (*Model 2*). This can be explained by the greater compliance of the shallower layers above the source, compared with the homogeneous case (*Model 0*). The numerical results for the uplift in the elastically homogeneous medium (*Model 0* and *Model 1*) are identical to the analytical point source solution. This confirms the conclusion derived from the dimensional analysis that the effect of the elasto-gravitational coupling on the displacement is negligible. The gravity change results (Fig. 4b) indicate that the contribution from the potential ϕ_p is negligible for all practical

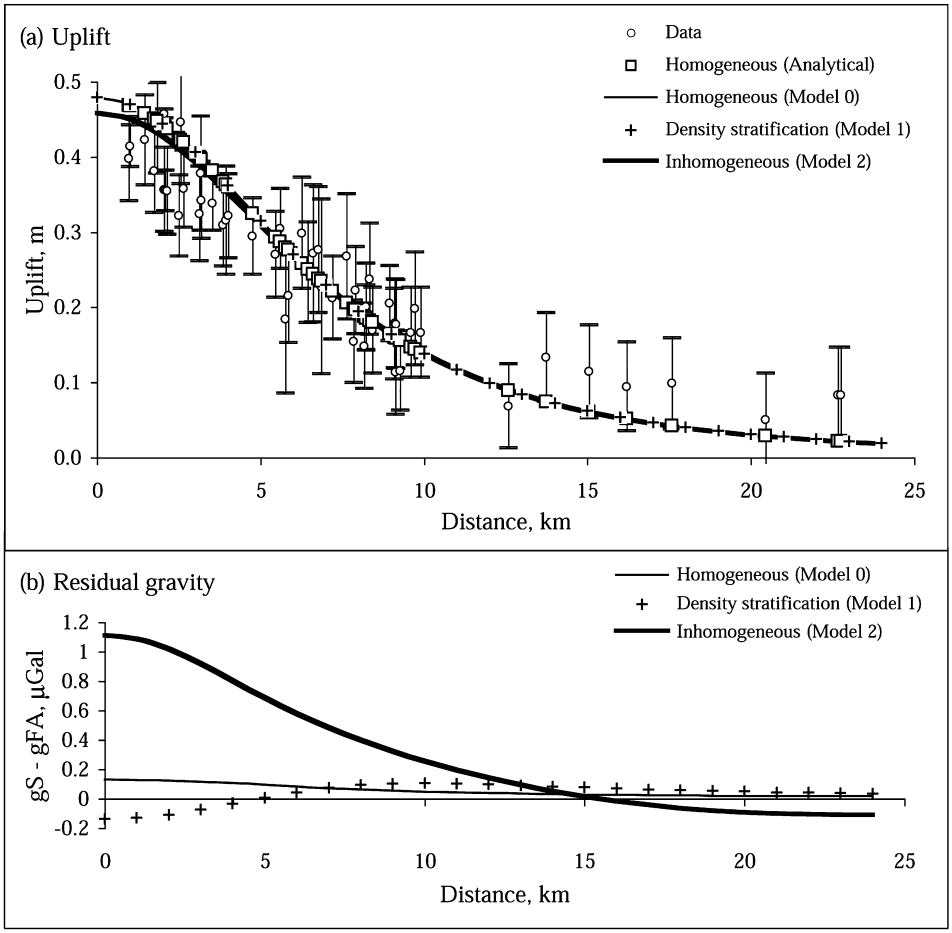

Figure 4

Pressurized massless cavity. (a) Match between experimental and modeled uplift. The plot shows no major differences between modeling the intrusion using a point source in a homogeneous or layered medium (see Table 3). (b) The plot shows the difference (residual gravity) between the surface gravity change (g_s) and the free-air effect (g_{FA}). The residual gravity corresponds to contributions to gravity changes from the elastic-gravitational coupling and density stratification. The maximum change (1 μGal) is about 3% of the residual gravity due to mass intrusion, well below the typical errors of 10 μGal for a relative gravity survey.

purposes. The numerical results for the elastically homogeneous media (*Model 0* and *Model 1*) show a maximum difference between the surface gravity and the free-air effect of less than 0.2 μGal (Fig. 4b). This is consistent with the numerical results of RUNDLE (1978) and the analytical results of WALSH and RICE (1979) that the change in gravity observed for a massless, spherically symmetrical, dilatational source in a homogeneous medium is equal to the free-air effect only, or $|\nabla V_p| = 0$. The contribution $|\nabla V_p|$ is practically negligible (about 1 μGal) in the inhomogeneous

Table 3

Results from numerical experiment

	Pressurized cavity				Mass intrusion			
	Depth km	Volume km^3	χ^2	R^2	Depth Km	Mass 10^{12} kg	χ^2	R^2
Point source (analytical)	8.8	0.16	57	0.99	8.8	0.45	37	0.66
Model 0 (homogeneous)	8.8	0.16	57	0.99	8.8	0.45	37	0.66
Model 1	8.8	0.16	57	0.99	8.8	0.45	37	0.66
Model 2 (inhomogeneous)	9.4	0.16	31	1.00	9.2	0.48	37	0.65

medium (*Model 3*, Fig. 4b) as well. Note that for a massless intrusion all the gravity changes (except the free-air effect) are well below the typical errors of 10 μGal (e.g., BATTAGLIA *et al.*, 1999).

The results for the case study of a point mass intrusion with no pressure change are very similar. The maximum displacement induced by the mass intrusion is around 3 mm (Fig. 5a), or about 1% of the uplift due to cavity pressurization, indicating that the contribution to the uplift from ∇V_p is practically negligible. The fit of the computed gravity changes to the Long Valley data (Fig. 5b, Table 3) do not show a significant difference between the three cases proposed. The estimated mass in the inhomogeneous medium (*Model 2*) is slightly larger (0.48×10^{12} kg instead of 0.45×10^{12} kg, a 7% increase) and deeper (9.2 km instead of 8.8 km, a 5% increase) than that inferred for the elastically homogeneous medium (*Model 0* and *Model 1*). The estimated density in the inhomogeneous medium (*Model 2*) is 7% higher (3000 kg/m^3 versus 2800 kg/m^3) than that for the elastically homogeneous medium (*Model 0* and *Model 1*).

4. Source Geometry

A very common approach to infer the deformation source parameters (depth, volume, mass, density) is to match gravity and uplift data to the predictions of an isotropic center of dilation (e.g., MOGI, 1958; EGGERS, 1987; MCKEE *et al.*, 1989; BERRINO, 1994; BATTAGLIA *et al.*, 1999; FERNÁNDEZ *et al.*, 2000; RYMER and WILLIAM-JONES, 2000). A major shortcoming of this technique is that we may fit the wrong model to the data, because different source models produce very similar vertical deformations (DIETERICH and DECKER, 1975). This may yield estimates of the density and depth of the intrusion that are not reliable. Consider, for example, modeling data generated from an ellipsoidal source (YANG *et al.*, 1988; CLARK *et al.*, 1986), assuming incorrectly a spherical symmetry for the source. The parameters of the actual ellipsoidal source are depth = 6 km, volume change = 0.2 km^3, mass change = 0.5×10^{12} kg and density = 2500 kg/m^3. The spherical source fits the uplift data well (see Fig. 6a) but predicts a deeper location for the intrusion (8.5 km

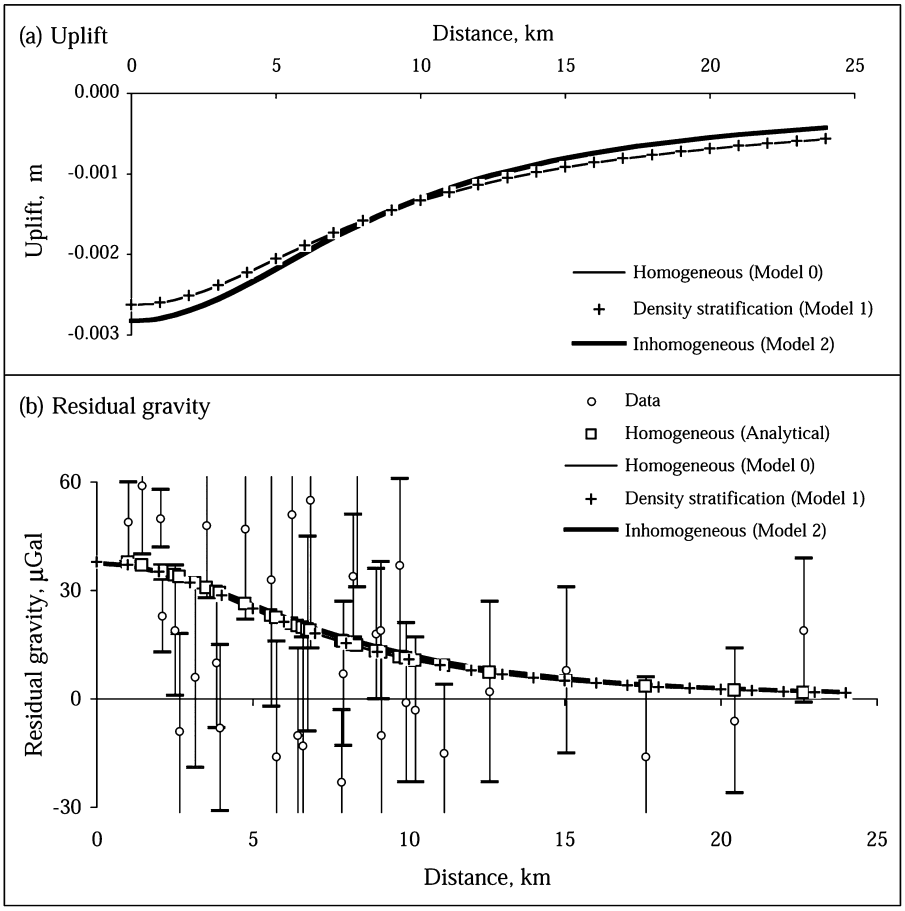

Figure 5
Spherical mass intrusion with no pressure change. (a) Uplift due to the mass intrusion. The maximum uplift (3 mm) is about 1% of the uplift due to cavity pressurization. (b) Match between experimental and modeled residual gravity. Again, the plot shows no major differences between modeling the intrusion using a point source in a homogeneous or layered medium (see Table 3).

instead of 6 km). The spherical model also requires a larger mass (0.9 instead of 0.5×10^{12} kg) to obtain the same gravity signal (Fig. 6b). The estimated volume increase is close to the correct value (0.2 km^3), because the spherical source is more efficient in causing vertical deformation. The spherical model fit appears reasonable and is able to explain about 99% of the uplift and gravity data. It is only when we compare the actual and computed radial displacements (Fig. 6c) that we realize that the spherical model is not appropriate. Using the parameters of the spherical source to estimate the intrusion density, we infer a value of 4500 kg/m^3 instead of the actual 2500 kg/m^3. Note that a straight line can successfully fit the ellipsoidal data gravity/height correlation as well (Fig. 6d). The linear correlation between gravity and height

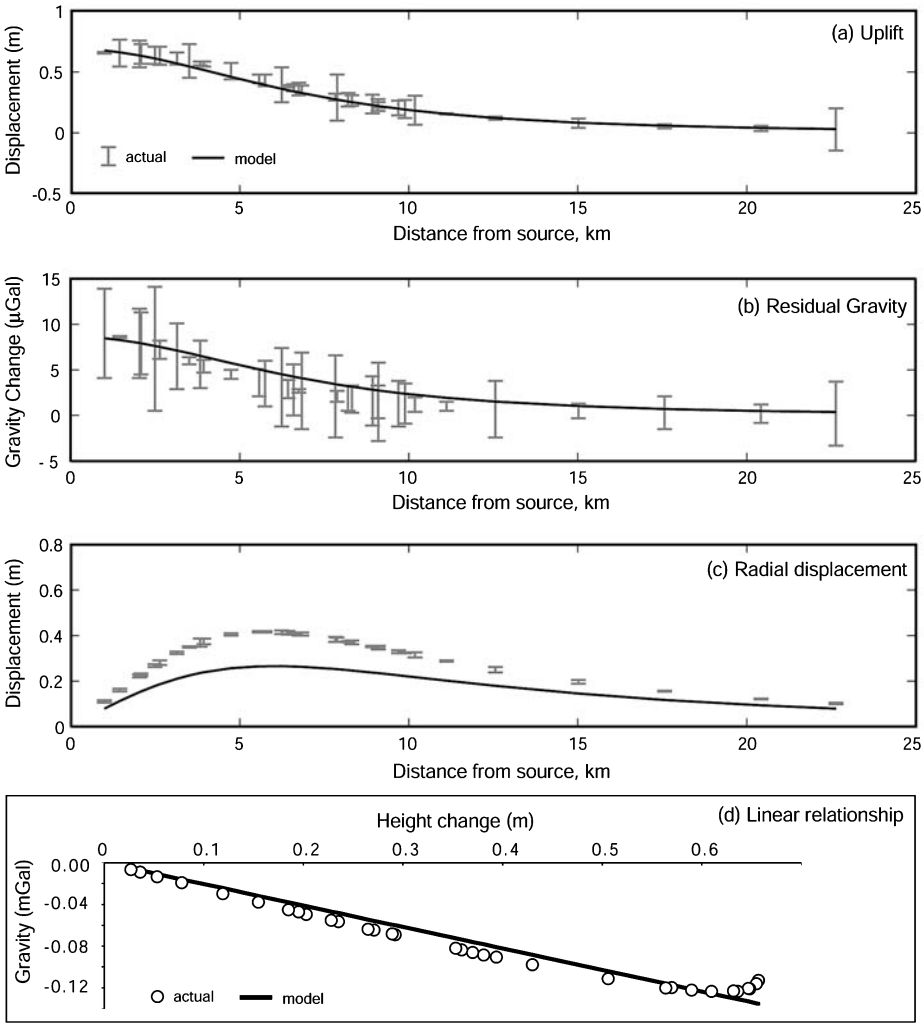

Figure 6

Bias due to incorrectly assessing the source shape. Actual ellipsoidal source (YANG *et al.*, 1988; CLARK *et al.*, 1986): depth = 6 km, volume = 0.2 km^3, mass = 0.5×10^{12} kg, density = 2500 kg/m^3. (a) (b) and (c) Fitting a spherical source (solid line) to a data set created using an ellipsoidal source (error bars). Uncertainties for the synthetic data set are 6 cm for uplift, 20 μGal for the residual gravity and 6 mm for the radial displacement. Inferred spherical source: depth = 8.5 km, volume = 0.2 km^3, mass = 0.9×10^{12} kg, density = 4500 kg/m^3. (d) A straight line fits the ellipsoidal data gravity/height correlation ($R^2 = 0.94$). The linear correlation between gravity and height changes is considered to be a special characteristic of spherically symmetric magma bodies (EGGERS, 1987). In this case, the inferred density is 3670 kg/m^3 and $\Delta g/\Delta u = 206 \pm 4$ μGal/m.

changes is considered to be a special characteristic of spherically symmetric magma bodies (EGGERS, 1987). In this case, the inferred density is 3670 kg/m^3 instead of the actual 2500 kg/m^3.

5. Summary and Conclusions

Combined geodesy and gravity measurements allow us to infer the density of intrusive bodies, and better constrain deformation sources in volcanic areas. In this work, we investigate three factors that can help in obtaining a more realistic picture of the intrusive body: (a) coupling between elastic and gravitational effects, (b) a layered Earth model, with one or more layers with differing densities and elastic properties and (c) non-spherical source geometries.

The first two factors investigated in this work do not affect the estimate of the source parameters significantly. Coupling between elastic and gravitational effects (self-gravitation) is second order over the time and distance scales normally associated with volcano monitoring. For a Maxwell material and at times long compared to the relaxation time, the stresses will relax to the point where the source terms are no longer balanced by the divergence of the stresses in the equilibrium equations. In this limit the self-gravitational effects cannot be ignored. We find no major differences between modeling the intrusion using a point source in a homogeneous or layered medium for an elastic model appropriate to Long Valley caldera.

Our results indicate that the critical step in the interpretation of the field data is the choice of the source model used to inverting geodetic and gravity data to infer the actual deformation source parameters. A simple experiment of matching deformation and gravity data from an ellipsoidal source using a spherical source shows that the standard approach of fitting a Mogi's source to gravity and uplift data only, excluding the horizontal displacements, can yield estimates of the source parameters that are not reliable. In our experiment, the spherical source fits the uplift and gravity data well (Figs. 6a and 6b), estimates correctly the volume increase (0.2 km^3), but predicts a deeper location (8.5 km instead of 6 km), a larger mass (0.9 instead of 0.5×10^{12} kg) and a larger density (4500 kg/m^3 instead of the actual 2500 kg/m^3) for the intrusion. Only by comparing the actual and the modeled radial displacements (Fig. 6c), we can demonstrate that the spherical model is not appropriate. It is important to note that a center of dilation can bias the results, overestimating the depth, mass and density of the intrusion. To obtain a reliable estimate of the depth and density of the intrusion, inversion of geodetic and gravity data should (a) not assume that the source possesses a spherical symmetry and (b) include not only the uplift and residual gravity, but the horizontal deformation as well (DIETERICH and DECKER, 1975). The ellipsoidal model can be used to invert geodetic and gravity data without assuming any particular orientation or symmetry, but the modeling requirements can be substantially more complicated than those for the Mogi's source (e.g., TIAMPO *et al.*, 2000).

Acknowledgements

We would like to thank J. Fernández for providing the numerical code. Reviews by F.H. Cornet and K.F. Tiampo greatly helped to improve the manuscript. Support for this research was provided by DoE, Office of Basic Energy Science, grant DE-FG03-99ER14962.

References

Aki, K. and Richards, P. G., *Quantitative Seismology: Theory and Methods* (W. H. Freeman and Co., San Francisco 1980).

Bailey, R. A. and Hill, D. P. (1990), *Magmatic Unrest at Long Valley Caldera, California*, 1980–1990, Geoscience Canada *17*, 175–179.

Battaglia, M., Roberts, C., and Segall, P. (1999), *Magma Intrusion beneath Long Valley Caldera Confirmed by Temporal Changes in Gravity*, Science *285*, 2119–2122.

Berrino, G., Rymer, H., Brown, G. C., and Corrado, G. (1992), *Gravity-height Correlations for Unrest at Calderas*, J. Volcanol. Geotherm. Res. *53*, 11–26.

Berrino, G. (1994), *Gravity Changes Induced by Height-mass Variations at the Campi Flegrei Caldera*, J. Volcanol Geotherm. Res *61*, 293–309.

Bonafede, M. and Mazzanti, M. (1998), *Modelling Gravity Variations Consistent with Ground Deformation in the Campi Flegrei Caldera* (*Italy*), J. Volcanol Geotherm. Res. *81*, 137–157.

Carle, S. (1988), *Three-dimensional Gravity Modeling of the Geologic Structure of Long Valley Caldera*, J. Geophys. Res. *93*, 13,237–13,250.

Cheng, C. H. and Johnston, D. H. (1981), *Dynamic and Static Moduli*, Geophys. Res. Lett. *8*, 39–42.

Clark, D. A., Saul, S. J., and Emerson, D. W. (1986), *Magnetic and Gravity Anomalies of a Triaxial Ellipsoid*, Exploration Geophysics *17*, 189–200.

Dawson, P. B., Evans, J. R., and Iyer, H. M. (1990), *Teleseismic Tomography of the Compressional Wave Velocity Structure beneath the Long Valley Region, California*, J. Geophys. Res. *95*, 11,021–11,050.

Dieterich, J. H. and Decker, R. (1975), *Finite Element Modeling of Surface Deformation Associated with Volcanism*, J. Geophys. Res *80*, 4094–4102.

Dvorak, J. J. and Dzurisin, D. (1997), *Volcano Geodesy: The Search for Magma Reservoirs and the Formation of Eruptive Vents*, Rev. Geophys. *35*, 343–384.

Eggers, A. (1987), *Residual Gravity Changes and Eruption Magnitudes*, J. Volcanol. Geotherm. Res. *33*, 201–216.

Fernández, J., Rundle, J., Granell, R., and Yu, T. (1997), *Programs to Compute Deformation due to a Magma Intrusion in Elastic-gravitational Layered Earth Model*, Comput. and Geosci. *23*, 231–249.

Fernández, J., Charco, M., Tiampo, K. F., Jentzsch, G., and Rundle, J. B. (2001a), *Joint Interpretation of Displacement and Gravity Data in Volcanic Areas. A Test Example: Long Valley Caldera, California*, Geophysic. Res. Lett. *28*, 1063–1066.

Fernández, J., Tiampo, K. F., Jentzsch, G., Charco, M., and Rundle, J. B. (2001b), *Inflation or Deflation? New Results for Mayon Volcano Applying Elastic-gravitational Modeling*, Geophysic. Res. Lett. *28*, 2349–2352.

Hill, D. P., Ellsworth, W. L., Johnston, M. S., Langbein, J. O., Oppenheimer, D. H., Pitt, A. M., Reasenberg, P. A., Sorey, M. L., and McNutt, S. R. (1990), *The 1989 Earthquake Swarm beneath Mammoth Mountain, California; an Initial Look at the 4 May through 30 September Activity*, Bull. Seismol. Soc. Am. *80*, 325–339.

Kissling, E., Ellsworth, W., and Cockerham, R. (1984), *Three-dimensional Structure of the Long Valley Caldera Region, California, by Geotomography*, Open-File Report - U.S. Geological Survey, OF *84–0939*, 188–220.

LANGBEIN, J., DZURISIN, D., MARSHALL, G., STEIN, R., and RUNDLE, J. (1995), *Shallow and Peripheral Volcanic Sources of Inflation Revealed by Modeling Two-color Geodimeter and Leveling Data from Long Valley Caldera, California, 1988–1992*, J. Geophys. Res. *100*, 12487.

LOVE, E. H., *Some Problems in Geodynamics* (Cambridge University Press, New York, 1911).

MCKEE, C., MORI, J., and TALAI, B., *Microgravity Changes and Ground Deformation at Rabaul Caldera, 1973–1985*. In IAVCEI Proc. in *Volcanology* (ed., Latter, J.) (Springer-Verlag, Berlin 1989), pp. 399–431.

MOGI, K. (1958), *Relations of the Eruptions of Various Volcanoes and the Deformation of Ground Surfaces around them*, Bull. Earthq. Res. Inst. Tokio Univ. *36*, 94–134.

POLLITZ, F. (1997), *Gravitational Viscoelastic Postseismic Relaxation on a Layered Spherical Earth*, J. Geophys. Res. *102*, 17,921–17,941.

PONKO, S. and SANDERS, C. (1994), *Inversion for P- and S-wave Attenuation Structure, Long Valley Caldera, California*, J. Geophys. Res. *99*, 2619–2635.

RUNDLE, J. (1978), *Gravity Changes and the Palmdale Uplift*, Geophys. Res. Lett. *5*, 41–44.

RUNDLE, J. (1982), *The Deformation, Gravity, and Potential Changes due to Volcanic Loading of the Crust*, J. Geophys. Res *87*, 10,729–10,744.

RYMER, H. (1994), *Microgravity Change as a Precursor to Volcanic Activity*, J. Volcanol. Geotherm. Res *61*, 311–328.

RYMER, H. and WILLIAMS-JONES, G. (2000), *Volcanic Eruption Precursors: Magma Chamber Physics from Gravity and Deformation Measurements*, Geophys. Res. Lett. *27*, 2389–2392.

SACKETT, P. C., MCCONNELL, V. S., ROACH, A. L., PRIEST, S. S., and SASS, J. H. (1999), *Long Valley coring Project, 1998—Preliminary Stratigraphy and Images of Recovered Core*, U.S. Geol. Survey Open-File Report 99–158.

SAVAGE, J. and COCKERHAM, R. (1984), *Earthquake Swarm in Long Valley Caldera, California, January 1983; Evidence for Dike Inflation*, J. Geophys. Res. *89*, 8315–8324.

SOREY, M. L., KENNEDY, B. M., EVANS, C. W., FARRAR, C. D., and SUEMNICHT, G. A. (1993), *Helium Isotope and Gas Discharge Variations Associated with Crustal Unrest in Long Valley Caldera, California, 1989–1992*, J. Geophys. Res *98*, 15,871–15,889.

TIAMPO K. F., RUNDLE, J. B., FERNÁNDEZ, J., and LANGBEIN J. (2000), *Spherical and Ellipsoidal Volcanic Sources at Long Valley Caldera, California, Using a Genetic Algorithm Inversion Technique*, J. Volcanol Geotherm. Res. *102*, 189–206.

YANG, X., DAVIS, P.M, and DIETERICH, J. H. (1988), *Deformation from Inflation of a Dipping Finite Prolate Spheroid in an Elastic Half-space as a Model for Volcanic Stressing*, J. Geophys. Res. *93*, 4249–4257.

WALSH, J., and RICE, J. (1979), *Local Changes in Gravity Resulting from Deformation*, J. Geophys. Res. *84*, 165–170.

ZHONG, S. and ZUBER, M. T. (2000), *Long-wavelength Topographic Relaxation for Self-gravitating Planets and its Implications for the Time-dependent Compensation of Surface Topography*, J. Geophys. Res. *105*, 4153–4164.

(Received November 12, 2002, revised January 31, 2003 accepted February 3, 2003)